ARTICLE
Journal of Cellular Biochemistry 117:470–482 (2016)

Journal of Cellular Biochemistry

F_1F_O ATP Synthase Is Expressed at the Surface of Embryonic Rat Heart-Derived H9c2 Cells and Is Affected by Cardiac-Like Differentiation

Marina Comelli,[1,2] Rossana Domenis,[1] Alessia Buso,[1] and Irene Mavelli[1,2]*

[1]*Department of Medical and Biological Sciences and MATI Centre of Excellence, University of Udine, p.le Kolbe 4, Udine 33100, Italy*

[2]*INBB Istituto Nazionale Biostrutture e Biosistemi, Viale Medaglie d'oro, Rome 00136, Italy*

ABSTRACT

Taking advantage from the peculiar features of the embryonic rat heart-derived myoblast cell line H9c2, the present study is the first to provide evidence for the expression of F_1F_O ATP synthase and of ATPase Inhibitory Factor 1 (IF_1) on the surface of cells of cardiac origin, together documenting that they were affected through cardiac-like differentiation. Subunits of both the catalytic F_1 sector of the complex (ATP synthase-β) and of the peripheral stalk, responsible for the correct F_1-F_O assembly/coupling, (OSCP, *b*, F6) were detected by immunofluorescence, together with IF_1. The expression of ATP synthase-β, ATP synthase-*b* and *F6* were similar for parental and differentiated H9c2, while the levels of OSCP increased noticeably in differentiated cells, where the results of *in situ* Proximity Ligation Assay were consistent with OSCP interaction within ecto-F_1F_O complexes. An opposite trend was shown by IF_1 whose ectopic expression appeared greater in the parental H9c2. Here, evidence for the IF_1 interaction with ecto-F_1F_O complexes was provided. Functional analyses corroborate both sets of data. i) An F_1F_O ATP synthase contribution to the exATP production by differentiated cells suggests an augmented expression of holo-F_1F_O ATP synthase on plasma membrane, in line with the increase of OSCP expression and interaction considered as a requirement for favoring the F_1-F_O coupling. ii) The absence of exATP generation by the enzyme, and the finding that exATP hydrolysis was largely oligomycin-insensitive, are in line in parental cells with the deficit of OSCP and suggest the occurrence of sub-assemblies together evoking more regulation by IF_1. J. Cell. Biochem. 117: 470–482, 2016.

KEY WORDS: ecto-F_1F_O ATP SYNTHASE; IF_1; OSCP; PLASMA MEMBRANE; CARDIAC-LIKE DIFFERENTIATION

For a long time F_1F_O ATP synthase was thought to exclusively locate in the inner mitochondrial membrane, generating energy by coupling the transmembrane delivery of protons to the synthesis of ATP [Stock et al., 1999]. However, many reports from several laboratories in recent years reported the location and function of the F_1F_O ATP synthase complex, or its component subunits, on the external surface of the plasma membrane. Various mammalian cell types have been investigated, including vascular endothelial cells, hepatocytes, adipocytes, myotubes, and tumor cells [Vantourout et al., 2010], as well as neural cells [Xing et al., 2012] and developing muscle cells [Garcia, 2011]. Plasma membrane F_1F_O-components, most usually β subunit, have been identified as receptors for multiple ligands, which combined with ecto-cellular ATP hydrolysis or ATP synthesis are involved in numerous biological processes. The most consolidated of these are control of intracellular pH, cholesterol homeostasis, and HDL endocytosis, regulation of endothelial cells proliferation/differentiation and angiogenesis, recognition of immune responses of tumor cells [Chi et al., 2006]. It has been also documented a role of the enzyme in regulation of calcium release especially during early development of myotubes [Garcia, 2011]. More recent evidence indicated that the cell surface ATP synthase is a binding protein for amyloid-β peptide (Aβ) on neural cells and suggested that the surface ATP synthase may be involved in oligomeric Aβ neurotoxic effects and neuro-degeneration [Xing et al., 2013]. Thus, the ectopic expression of F_1F_O ATP synthase (ecto-F_1F_O ATP synthase) is now widely recognized, but nothing has been reported so far about cells of cardiac origin. The idea that its subunit organization is the same as the mitochondrial enzyme is accepted based on several suggestions [Wang et al., 2006; Ma et al., 2010; Rai et al., 2013]. Of note, a characterization of the

Conflict of interest: None.
Grant sponsor: University of Udine.
*Correspondence to: Prof. Irene Mavelli, Department of Medical and Biological Sciences, University of Udine, p.le Kolbe 4, 33100 Udine, Italy. E-mail: irene.mavelli@uniud.it
Manuscript Received: 22 January 2015; Manuscript Accepted: 29 July 2015
Accepted manuscript online in Wiley Online Library (wileyonlinelibrary.com): 30 July 2015
DOI 10.1002/jcb.25295 • © 2015 Wiley Periodicals, Inc.

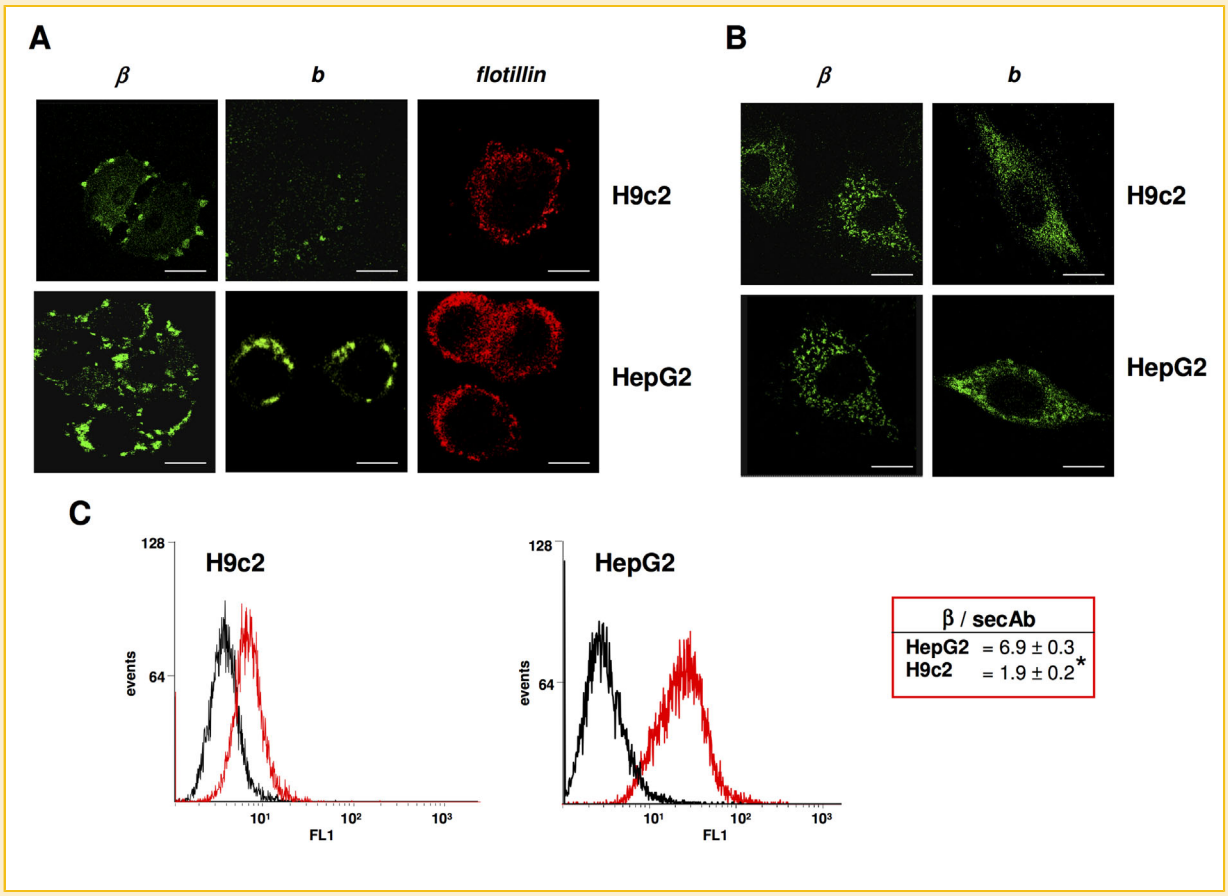

Fig. 1. Ectopic expression of β and *b* subunits of F_1F_O ATP synthase in H9c2 cells *vs* HepG2 cells. (A, B) Confocal microscopy analysis of intact (A) and permeabilized (B) cells for ATP synthase-β and ATP synthase-b. Profiles of intact cells were stained with polyclonal antibody anti-flotillin. Representative images of three separate experiments were reported. Bars = 30 μm. (C) Histogram plot of flow cytometry for ATP synthase-β. Black traces (left histograms) show cells incubated with only the secondary antibody and red traces (right histograms) cells labelled with monoclonal anti−β antibody. One experiment representative of three is shown. The mean fluorescence values relative to their own negative controls are reported in the insert (mean ± SD; n = 3; $^*P < 0.001$). Experimental procedures are in Methods.

complex of plasma membranes from rat liver was recently provided, documenting that it has a similar molecular weight to the monomeric form of the mitochondrial complex and contains not only nuclear but also mitochondrially-encoded subunits [Rai et al., 2013]. The authors concluded that this finding makes it unlikely that the enzyme assembles on the plasma membranes, but suggests it to be transported from mitochondria by still unknown pathways, in accordance with previous reports [Wang et al., 2006; Ma et al., 2010].

The mitochondrial F_1F_O ATP synthase presents a hydrophobic membrane domain, F_O, containing a H^+ channel in proximity of the interface between the *c*-ring and the associated *a*-subunit, and a hydrophilic domain, F_1 ($\alpha_3\beta_3$ subunits), bearing the adenine nucleotide processing sites. F_O and F_1 domains are connected by the so-called central (γ, δ, ε subunits) and peripheral stalks [Baker et al., 2012]. The peripheral stator stalk consists of single copies of oligomycin-sensitivity conferral protein (OSCP), *b*,*d* and *F6* subunits. It associates with the apex of the F_1 domain through OSCP and extends along the periphery of the F_1, running along an α/β-interface, into the membrane domain of the enzyme. Thus, the peripheral stator stalk enters the lipid bilayer throughout the membrane-bound portion of subunit *b*, that is the only subunit observed to span the soluble and membrane-embedded parts of the stalk. The mitochondrial enzyme contains also the ATPase Inhibitory Factor 1 (IF_1), which is a basic protein that reversibly binds to one of the three β subunits thereby inhibiting the enzyme [Green and Grover, 2000; Bason et al., 2011]. IF_1 functions in mitochondrial membrane as a regulatory protein and binds in response to decrease in pH and/or under conditions favoring the ATPase mode of the enzyme functioning, for example at low transmembrane potential as occurs under cardiac ischemia or after preconditioning [Green and Grover, 2000; Di Pancrazio et al., 2004]. IF1 also binds when the enzyme complex is partially uncoupled or sub-assemblies are present in mitochondrial membranes [Carrozzo et al., 2006; Mourier et al., 2014]. IF_1 is expressed even on the external surface of endothelial [Cortes-Hernandez et al., 2005; Martinez et al., 2015] and hepatic cells [Contessi et al., 2007; Mangiullo et al., 2008; Giorgio et al., 2010; Martinez et al., 2015], as well as in myelin vesicles [Ravera et al., 2011]. On the cell surface IF_1 function might be not

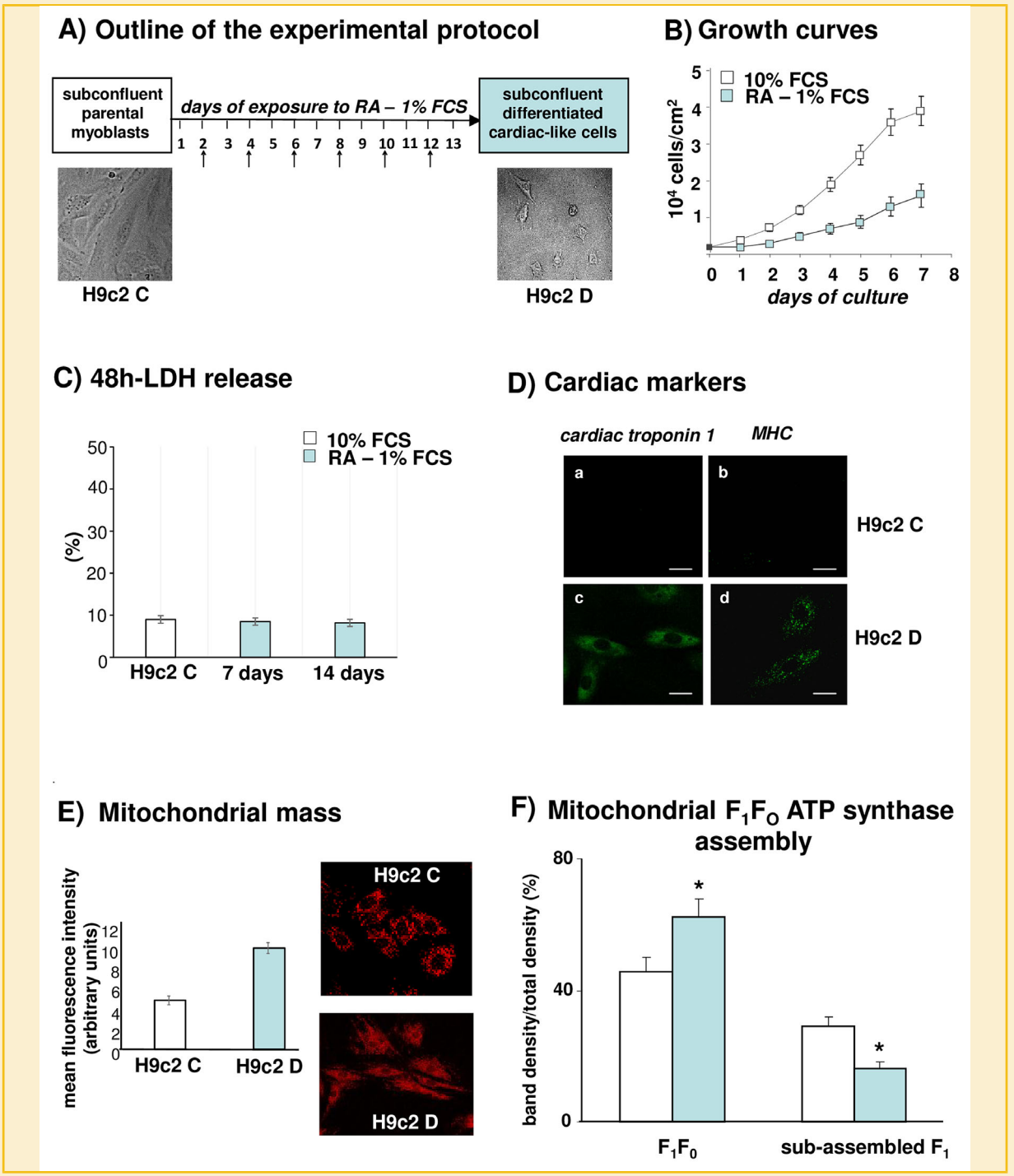

Fig. 2. Overall description of H9c2 cardiac-like differentiation protocol and some relevant changes occurring alongside. (A) Outline of the experimental protocol. RA = *all-trans*-retinoic acid; FCS = fetal calf serum; the arrows indicate the days of the medium replacement during cell culturing under differentiating conditions. (B) Growth curves. Data (cells/cm^2) were from Trypan Blue dye exclusion tests and represent means ± SD of four different experiments. Cells were followed until seven days of culture in normal (10% FCS) or in differentiating (RA-1% FCS) conditions. (C) 48 h-LDH release. 48 h-LDH release indicates the release of LDH in the growth medium during 48 h of culture, before the medium replacement. The values are expressed as a percentage of the total LDH activity of the cells: that is extracellular LDH/(extracellular LDH + intracellular LDH). Data represent means ± SD of three different experiments. (D) Cardiac markers analyzed by confocal microscopy. Images of parental myoblasts (H9c2 C) and differentiated cardiac-like cells (H9c2 D) were selected from three different experiments (Bar = 30 μm). MHC = myosin heavy chain. (E) Changes in mitochondrial mass by flow cytometry and confocal microscopy analyses. Parental myoblasts (H9c2 C) and differentiated cardiac-like cells (H9c2 D) were probed with mitotracker red. The histograms represent the mean fluorescence intensity of three different experiments (means ± SD). Pictures are confocal images selected from three different experiments. (F) Changes in assembly of mitochondrial F_1F_O ATP synthase in membrane. BN-PAGE (4–11%) analysis of n-dodecylmaltoside (DDM) mitochondrial extracts for the fully assembled enzyme complex F_1-F_O and the sub-assembled F_1 in H9c2 C (white columns) and in H9c2 D cells (light blue/gray columns). Data are from Comelli et al., 2011.

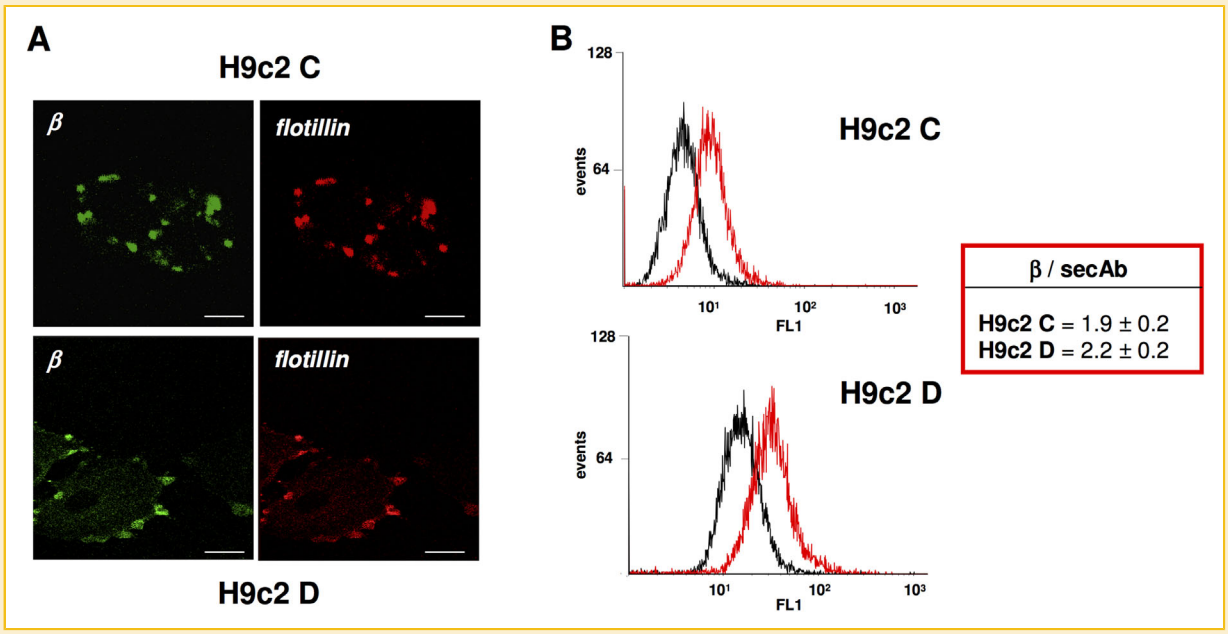

Fig. 3. Expression of F_1F_O ATP synthase-β on the surface of H9c2 cells induced to cardiac-like differentiation. (A) Parental (H9c2 C) and differentiated (H9c2 D) intact cells were treated with monoclonal anti-β or polyclonal anti-flotillin antibody and analyzed by confocal microscopy. Representative images of three separate experiments were reported. Bars = 30 μm. (B) Histogram plot of flow cytometry for H9c2 C and H9c2 D cells labelled with only the secondary antibody (black traces/left histograms), or with anti−β antibody (red traces/right histograms). One experiment representative of three is shown. The relative mean fluorescence values are reported in the insert (mean ± SD). Experimental procedures are in Methods.

limited to regulation of F_1F_O ATP synthase [Cortes-Hernandez et al., 2005] and it might interact with different target proteins such as calmodulin [Contessi et al., 2007].

A main goal of the present study was to investigate whether ecto-F_1F_O ATP synthase is expressed on H9c2 myoblasts, considering the extensive application of this cell line as a model for cardiac cells in a multiplicity of studies [Pereira et al., 2011 and references therein; Kuznetsov et al., 2015]. Indeed, H9c2 myoblasts are derived from the ventricular part of embryonic rat heart and, although are not true cardiac cells, they possess similar morphological, electrophysiological, and biochemical properties, for example energy metabolism, to primary cardiomyocytes [Hescheler et al., 1991, Kuznetsov et al., 2015], while maintain characteristics of immature embryonic cells [Kageyama et al., 2002].

We used immunofluorescence approaches and enzymatic activity measurements allowing us to get evidence on intact and viable cells. Our findings are consistent with the expression on the external surface of H9c2 cells of F_1F_O ATP synthase subunits that are part of the F_1 domain or of the peripheral stator stalk, including β, OSCP, *b*, and *F6*, as well as of the regulatory protein IF_1.

It is worth mentioning that proliferating H9c2 myoblasts can be differentiated towards a more cardiomyocyte-like phenotype by culturing cells in reduced serum medium containing *all-trans*-retinoic acid. We recently reported that these conditions induce the appearance of cardiomyocyte-like ultrastructural features and enhance the assembly of mitochondrial F_1F_O ATP synthase along with mitochondria biogenesis and remodelling [Comelli et al., 2011; Bisetto et al., 2013]. Thus, a primary aim of this study was also to compare proliferating and differentiating H9c2 cells focusing on ecto-F_1F_O ATP synthase. Overall, the results provide evidence for an increase of catalytically competent and well assembled/coupled F_1F_O complexes on cell surface of H9c2 along with the acquisition of the more cardiomyocyte-like phenotype.

MATERIALS AND METHODS

CELL CULTURES AND MATERIALS

H9c2 embryonic rat heart-derived myoblasts (ATCC CRL-1446), purchased from the American Type Culture Collection, were grown as in [Comelli et al., 2011]. Sub-confluent cells (70–80%) were sub-cultured to prevent low serum-culturing and loss of myoblastic cells. In fact, H9c2 myoblasts can rapidly lose their characteristics and undergo spontaneous trans-differentiation, becoming multi-nucleated myotubes, under conditions of decreased serum concentration and of achieved confluence [Menard et al., 1999].

H9c2 cells were also cultured in reduced serum medium containing *all-trans*-retinoic acid (RA) as in [Comelli et al., 2011], to induce differentiation of the parental line toward cardiac-like phenotype, with the medium being replaced every 2 days. Cytotoxicity was monitored by a sensitive LDH release assay following manufacturer's instructions (Cytotox 96 non-radioactive assay kit, Promega, Medison, WI).

Human hepatocarcinoma HepG2 cells (ATCC HB8065) were grown as in [Contessi et al., 2007].

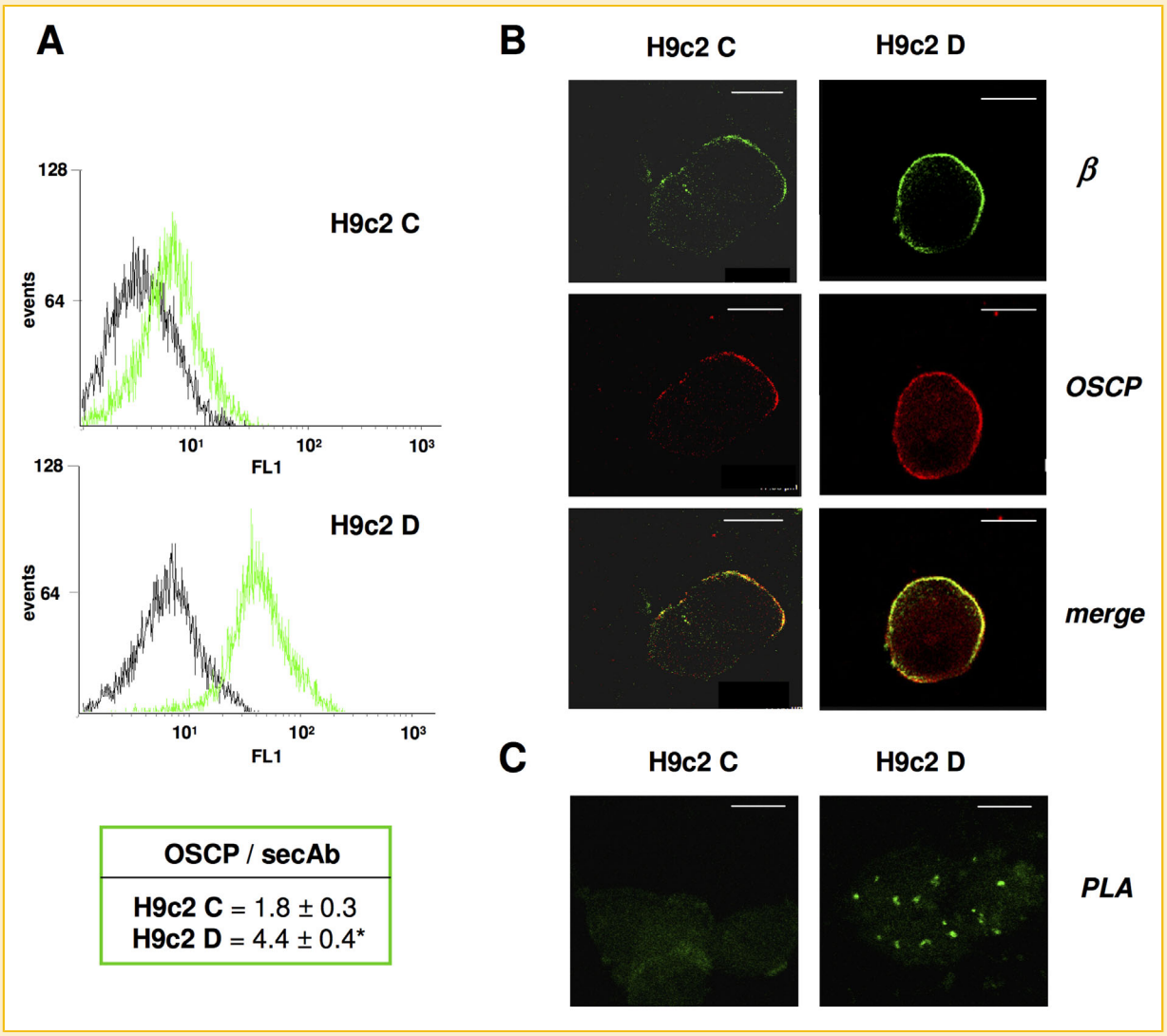

Fig. 4. Effect of H9c2 cardiac-like differentiation on the ectopic expression of F_1F_O ATP synthase OSCP subunit. Parental (H9c2 C) and differentiated (H9c2 D) cells were treated and analyzed by cytofluorimetry and confocal microscopy (cell surface immunostaining and in situ PLA assay) as described in Methods. (A) Cytofluorimetry histogram plots: black traces (left histograms) indicate cells incubated in the presence of only the secondary antibody and green traces (right histograms) cells incubated with anti-OSCP antibody. One experiment representative of three is shown. The mean fluorescence values relative to their own negative controls are reported in the insert (mean ± SD; n = 3; $^*P < 0.001$). (B) Confocal microscopy analysis of live cells doubly labelled with monoclonal anti-β and polyclonal anti-OSCP antibody. The merged image indicates colocalization of the two fluorophores. Representative images of three separate experiments were reported. Bars=30 μm. (C) Images from in situ PLA assay used to demonstrate β-OSCP interaction. Distinct fluorescent dots (PLA signals), indicating the occurrence of interaction, are evident in H9c2 D. Representative images of three separate experiments were reported. Bars =30 μm.

All the experiments were done with cells not approaching confluence.

All chemicals and reagents were purchased from Sigma (St. Louis, MO), unless specifically indicated.

IMMUNO-BASED ASSAYS

The primary antibodies were: rabbit polyclonal and mouse monoclonal antibody anti-β (Abcam, Cambridge, UK); rabbit polyclonal anti-α/β kindly provided by dr. F. Dabbeni-Sala, Department of Pharmacology, University of Padua, Italy); mouse monoclonal anti-IF_1 (Santa Cruz Biotecnology, Inc., CA); mouse monoclonal anti-OSCP (Abcam, Cambridge, UK); mouse monoclonal anti-*F6* (Abcam, Cambridge, UK); rabbit polyclonal anti-*b* (Proteintech Europe, Manchester, UK); rabbit polyclonal anti-flotillin 1 (Abcam, Cambridge, UK).

FITC-conjugated rabbit anti-mouse IgG or TRIC-conjugated goat anti-rabbit IgG (Chemicon International, Temecule, CA) were used as secondary antibodies.

Parental and differentiated cells were tested together in order to avoid possible differences in efficacy of the antisera. Cells treated with only secondary antibody served as negative controls.

CONFOCAL MICROSCOPY

5×10^4 cells were plated in complete growth medium on glass coverslips, grown overnight, and treated as in [Contessi et al., 2007].

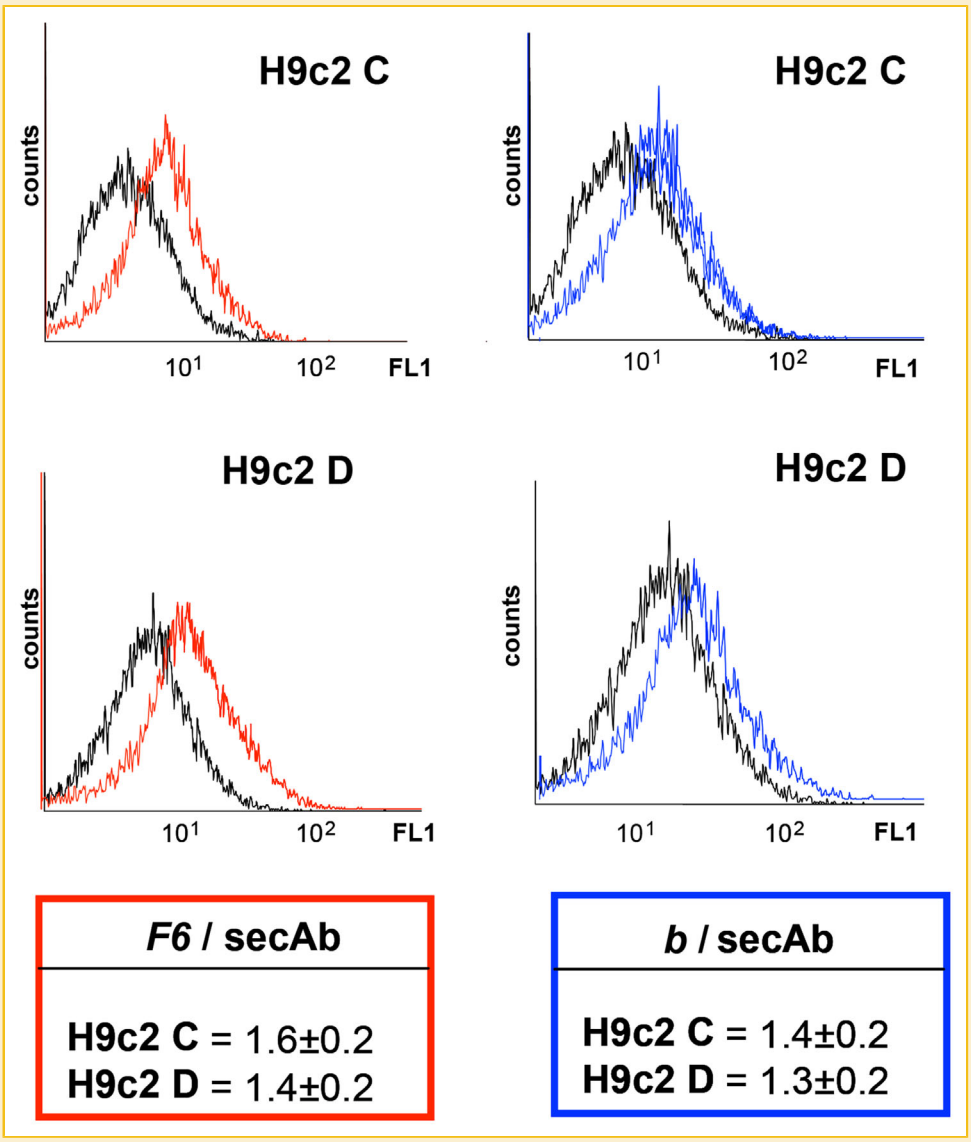

Fig. 5. Flow cytometry analysis of the ectopic expression of ATP synthase F_6- and *b*-subunits in parental and cardiac-like differentiated H9c2. Parental (H9c2 C) and differentiated (H9c2 D) cells were treated and analyzed by cytofluorimetry as described in Methods. Histogram plots: black (left) traces indicate cells incubated in the presence of only the secondary antibody, red or blue (right) traces cells incubated with anti-*F6* or anti-*b* antibody. One experiment representative of three is shown. The mean fluorescence values relative to their own negative controls are reported in the inserts (mean ± SD; n = 3; $^*P < 0.001$).

Briefly, cells fixed with 3.7% paraformaldehyde in phosphate-buffered saline pH 7.4 (PBS) were washed three times with PBS and treated with (permeabilized cells) or without (intact, non-permeabilized cells) 0.2% Triton X-100 for 5 min. Cells were then incubated for 3 h in blocking solution (1% bovine serum albumin in PBS) at room temperature with primary antibodies. After three washings with PBS, cells were stained for 2 h at room temperature with FITC-conjugated or TRIC-conjugated IgG. After washings, the coverslips were mounted in glycerol-based mounting fluid (Chemicon International), and examined with a laser scanning microscope equipped with a 488–534 nm Ar laser and a 633 nm He-Ne laser (Leica TCS NT, Leica Mycrosystems, Wetzlar, Germany) by confocal optical sections taken through the z-axis. Five microscope fields per slide (at least two slides) were viewed for each group analysed. The cells showed a staining pattern symptomatic of homogeneous populations. An accurate setting of the instrument allowing to minimize spectral overlap was made in order to evaluate the merged images correctly. The specificity of the immunostaining pattern was confirmed by verifying that no staining was observed in control cells treated with only secondary antibodies.

IN SITU PROXIMITY LIGATION ASSAY (PLA)

To analyse the protein–protein interaction, we used the in situ PLA technology Olink Bioscience (Uppsala, Sweden) following manufacturer's instructions. Briefly, this method utilizes dual target recognition of two proteins that putatively interact, and consists of a pair of primary antibodies raised in different species and two

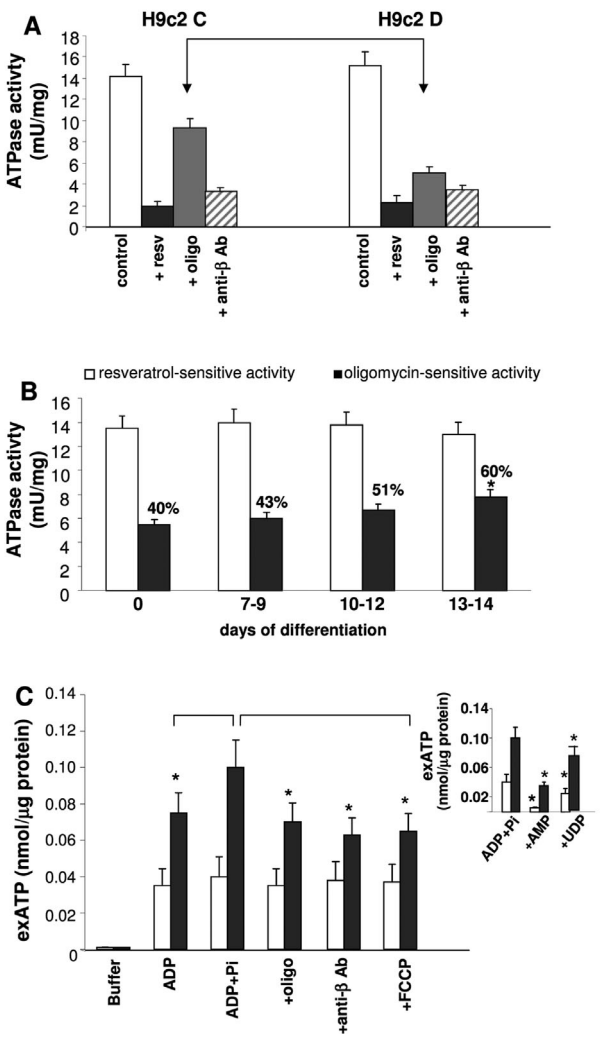

Fig. 6. exATP hydrolysis rate and exATP production by ecto-F_1F_O ATP synthase on cell surface of H9c2 and effect of cardiac-like differentiation. (A) Maximal exATP hydrolysis rate by intact parental (H9c2 C) and differentiated (H9c2 D) cells was analyzed by a spectrophotometric coupled pyruvate kinase/lactate dehydrogenase assay, in the absence or in the presence of the indicated inhibitors (20 μM resveratrol, 10 μM oligomycin, 1:100 anti-β Ab). Values represent means ± SD of three different experiments. The arrows mark the only significant difference observed ($P < 0.01$) in H9c2 D *vs* H9c2 C. (B) Ecto-ATPase activity (resveratrol-sensitive) and ATPase activity of holo-F_OF_1 ATP synthase (oligomycin-sensitive) by intact cells were analyzed during the differentiation protocol. Values represent means ± SD of three different experiments. (C) Ex-ATP production was measured in parental (white columns) and differentiated H9c2 (black columns), incubated with buffer alone (buffer), or with buffer plus ADP (ADP), or with buffer plus ADP and Pi (ADP+Pi). After 30 s the medium samples were collected and ATP measured by luciferin-luciferase assay. Measurements in the presence of (ADP+Pi) were also made after 15 min pretreatment with specific inhibitors: 10 μM oligomycin (oligo), AMP (11 mM) (in the insert), UDP (2 mM) (in the insert), FCCP (25 μM) and anti-β antibody (1:100). Basal ex-ATP levels in the absence of ADP (buffer) produced bioluminescence signals <3% of the uninhibited levels in the presence of ADP+Pi. Three separate experiments were performed in triplicate. Data shown are means ± S.D., n = 3, $^*P < 0.01$ vs. ADP+Pi. Experimental procedures are in Methods and *Supporting Information*.

different secondary antibodies conjugated with oligonucleotides (PLA probes). If the two antibodies bind epitopes that are in close proximity on interacting proteins, the oligonucleotides will also be brought into proximity and form a DNA circle that will be replicated using rolling circle amplification (RCA). The RCA product, made of fluorophore-labeled oligonucleotides, can be easily detected by confocal microscopy as a brightly fluorescent, submicrometer-sized spot (PLA signal) [Leuchowius et al., 2010]. Technical controls, represented by the omission of primary antibodies, resulted in the complete loss of PLA signal. Cells were visualized through a Leica TCS SP laser-scanning confocal microscope (Leica Microsystems, Wetzlar, Germany).

FLOW CYTOMETRY

Sub-confluent cells were washed twice in PBS, and treated as in [Contessi et al., 2007]. Briefly, cells detached with trypsin-EDTA were fixed with 3.7% paraformaldehyde in PBS for 15 min, and washed twice in blocking solution (PBS containing 1% BSA). Fixed cells were incubated in blocking solution with primary antibodies at 20°C for 1 h. The cells were then washed in PBS and incubated with FITC-conjugated IgG at 20°C for 30 min. After washings in PBS, cells were suspended at a concentration of 2×10^6 cell/ml in PBS and analyzed with a FACScan flow cytometer (Becton–Dickinson, New York) equipped with a single argon laser at 488 nm (excitation wavelength). The emission was monitored at 530 nm (FL-1 green fluorescence). The scatter plot showed a homogeneous cell population with no dead cells or debris for all the analyzed conditions. Data were acquired in list mode and analyzed with CellQuest Software (Becton–Dickinson, New York). 10,000 cells were analyzed per group.

EXTRACELLULAR ATP HYDROLYSIS ASSAY

The rate of extracellular ATP (exATP) hydrolysis by intact cells was measured by an enzyme-coupled assay with ATP-regenerating system according to [Comelli et al., 2011], using an UV plate reader equipped with a 340 nm filter (EL 808, Bio-Tek Instruments Inc., Winooski, VT). Cell suspensions were pre-incubated 15 min at room temperature with or without inhibitors. For details, see *Supporting Material*.

EXTRACELLULAR ATP PRODUCTION

Adherent cells were pre-incubated 15 min at 37°C with or without inhibitors, 50 μM ADP alone or plus 5 mM Pi was added and exATP generated after 30 s was measured using the ATP bioluminescence kit ATPlite (Perkim Elmer, Groningen, The Netherlands), following manufacturer's instructions. Luminescence was measured in a microplate luminometer (Modulus II-Turner Biosystems). After the assay, viability was monitored in each microplate well by Trypan blue test. For details, see *Supporting Material*.

STATISTICAL ANALYSIS

Data are reported as means ± S.D. Intergroup comparison were made using unpaired two-tailed Student's *t*-test. Values of $P > 0.05$ were considered as not statistically significant and were not indicated.

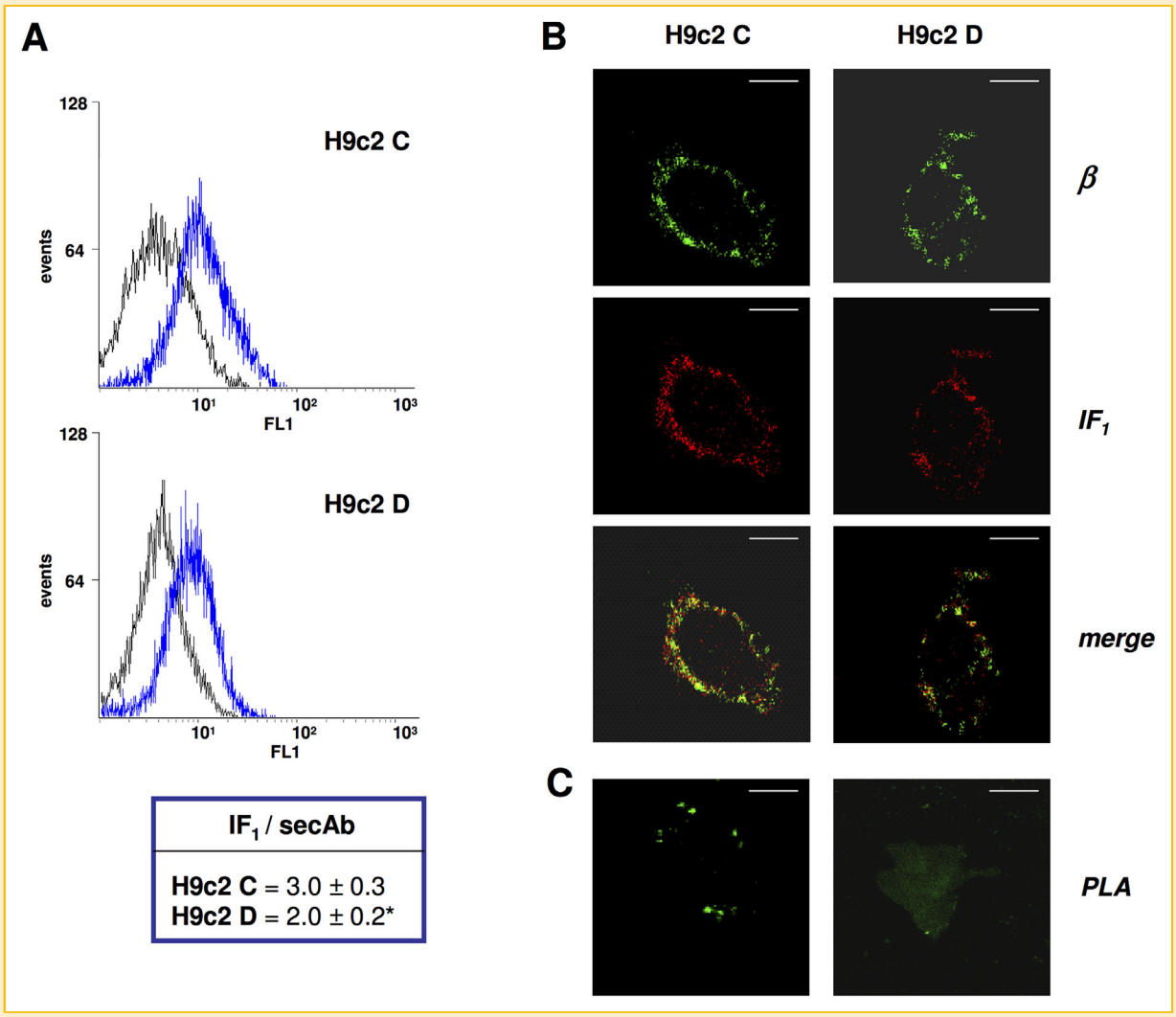

Fig. 7. IF_1 expression on the surface of H9c2 cells and interaction with ecto-F_1F_O ATP synthase are affected by cardiac-like differentiation. Parental (H9c2 C) and differentiated (H9c2 D) cells were treated and analyzed by cytofluorimetry and confocal microscopy (cell surface immunostaining and *in situ* PLA assay) as described in Methods. (A) Citofluorimetry histogram plots: black traces (left histograms) indicate cells incubated in the presence of only the secondary antibody and blue traces (right histograms) cells incubated with anti-IF_1 antibody. One experiment representative of three is shown. The mean fluorescence values relative to their own negative controls are reported in the insert (mean ± SD; n = 3; $^*P < 0.01$). (B) Confocal microscopy analysis of live cells doubly labelled with monoclonal anti-β and polyclonal anti-IF_1 antibody. The merged image indicates colocalization of the two fluorophores. Representative images of three separate experiments were reported. Bars=30 μm. (C) Images from *in situ* PLA assay used to demonstrate the IF_1-β interaction. Distinct fluorescent dots (PLA signals), indicating the occurrence of interaction, are evident in H9c2 C. Representative images of three separate experiments were reported. Bars = 30 μm.

RESULTS AND DISCUSSION

F_1F_O ATP SYNTHASE ON THE SURFACE OF EMBRYONIC RAT HEART-DERIVED H9C2 CELLS

We tested for the presence of ecto-F_1F_O ATP synthase embryonic rat heart-derived H9c2 cells using immunofluorescence. We compared the data with hepatic HepG2 cells where an abundant ecto-cellular expression of the enzyme was well documented, and its subunit composition was thoroughly investigated [Bae et al., 2004; Contessi et al., 2007; Kim et al., 2010]. Analyses were carried out for two subunits with different properties, that is the hydrophilic ATP synthase-β, that is part of the catalytic F_1 sector, and the partially hydrophobic ATP synthase-*b*, assigned to the peripheral stator stalk. Subunits of F_O domain were not investigated taking into account the challenging immunostaining of such subunits, which are largely hydrophobic and membrane-embedded. In H9c2 cells the ectopic expression was well detectable for ATP synthase-β and hardly visible but not negligible for ATP synthase-*b* (Fig. 1A, upper pictures), compared to HepG2 where they were both well detectable (Fig. 1A, lower pictures). The focus of the analysis in Figure 1 was to demonstrate the localization on the cell surface of the two ATP synthase subunits by the accessibility of externally added

antibodies, while flotillin served to label cell profile (Fig. 1A). Non-permeabilized cells showed a patchy and punctuate staining pattern resembling cell profile and suggesting that ATP synthase-β and ATP synthase-*b* localize to plasma membrane in H9c2, as for HepG2 cells [Contessi et al., 2007]. Immunostaining of flotillin, a marker of lipid rafts, showed an analogous patchy and punctuate pattern (Fig. 1A). This was in accordance with the localization of ecto-F_1F_O ATP synthase in lipid rafts from plasma membranes reported for several cell types [Bae et al., 2004; Wang et al., 2006; Kim et al., 2010; Raj et al., 2013]. Absence of immunofluorescence signal in cells treated with only secondary antibody (*Supplementary Fig. 1 and 2*) indicated that the staining pattern was specific for ATP synthase-β or ATP synthase-*b*. Indeed, no cross-reactions were expected due to the high specificity of the primary antibodies, as verified by immunoblotting analyses of detergent-extracts of the cells (not shown). When cells were doubly labelled with anti-β and anti-*b* antibodies, even if the staining for ATP synthase-*b* was little appreciable, the merged image displayed a yellowish-orange punctuate staining, mainly matching ATP synthase-*b* brighter spots, and recalling co-localization of the two subunits (*Supplementary Fig. 3)*. Of note, parallel experiments run on permeabilized cells showed for both β and *b* subunits a very different pattern, typical of mitochondrial staining with a characteristically tubular/reticular appearance (Fig. 1B).

In conclusion, we are confident that both ATP synthase-β and ATP synthase-*b* localize on the cell surface of H9c2, though ATP synthase-*b* is only just observable if compared to ATP synthase-β. As the subunit organization of the ecto-F_1F_O complex should reflect that of the mitochondrial complex [Yonally et al., 2006; Wang et al., 2006; Ma et al., 2010; Rai et al., 2013], the low immunostaining of ATP synthase-*b* may be ascribed to its low accessibility. Indeed, based on the known structure of the peripheral stator stalk of the mitochondrial enzyme [Rees et al., 2009; Baker et al., 2012], a very extensive area of the membrane extrinsic region of subunit *b* is buried from its interactions with subunits *d* and *F6*. Nevertheless, considering the well detectable immunofluorescence staining observed in mitochondria (Fig. 1B), as well as on HepG2 cell surface (Fig. 1A), which is in line with a high expression of F_1F_O ATP synthase, we can state that the hardly visible ATP synthase-*b* signal is consistent with low levels of F_1F_O ATP synthase.

We validated confocal microscopy data by cytofluorimetric analyses and quantified the expression of ATP synthase-β on the cell surface of H9c2 with reference to HepG2 cells (Fig. 1C). For both cell types data showed a noticeable increase in the mean fluorescence intensity when cells were labelled with anti-β antibody, relative to that observed omitting the primary antibody. The values for H9c2 were 3.6-fold lower than HepG2, in line with a lower ectopic expression of F_1F_O ATP synthase for non-tumoral cells [Bae et al., 2004; Yonally et al., 2006; Mangiullo et al., 2008; Rai et al., 2013; Wang et al., 2013].

EFFECTS OF CARDIAC-LIKE DIFFERENTIATION ON THE ECTO-F_1F_O ATP SYNTHASE EXPRESSION

Proliferating H9c2 myoblasts are not fully differentiated cardiac cells and can be differentiated towards a more cardiomyocyte-like phenotype by culturing cells in reduced serum medium containing *all-trans* retinoic acid. These conditions promote the expression of L-type Ca^{2+} channel and troponin 1 and induce the appearance of cardiomyocyte-like ultrastructural features [Menard et al., 1999; Comelli et al., 2011]. Cells induced to differentiate towards the more cardiomyocyte-like phenotype were recently validated as a good model to investigate the cardioprotective and cardiotoxic actions of quercetin and its in vivo metabolites [Daubney et al., 2015].

We decided to verify the hypothesis that in differentiated H9c2 cells well assembled/coupled F_1F_O ATP synthase complexes would be present in greater amount at cell surface, as already observed in mitochondria [Comelli et al., 2011; Bisetto et al., 2013]. With this aim, we induced H9c2 cells to differentiate towards the cardiac lineage and monitored by immunofluorescence the effects on ecto-F_1F_O ATP synthase. The overall description of the differentiating treatments was outlined in Figure 2, together with some characteristics acquired by the cells and relevant for the discussion of the results (i.e., growth rate, cardiac markers, mitochondrial mass, and mitochondrial F_1F_O ATP synthase assembly). During the treatment, cytotoxicity was verified by a sensitive LDH-release assay, as widely reported for several cell systems [Jurisic, 2003; Jurisic et al., 2004]. Very low treatment cytotoxicity was observed (Fig. 2C) after either 7 ($8.5 \pm 0.1\%$) or 14 days ($8.2 \pm 0.2\%$), similar to that of proliferating parental cells ($9.0 \pm 0.1\%$). We focused on the catalytic subunit ATP synthase-β together with three subunits composing the peripheral stator stalk, which is responsible for the correct F_1-F_O assembly/coupling, specifically OSCP, *b*, and *F6*. Confocal microscopy analysis for ATP synthase-β (Fig. 3A) showed a patchy and punctuate staining pattern, resembling flotillin, in both parental (upper pictures) and cardiac-like differentiated (lower pictures) cells. Quantification by cytofluorimetric analysis showed very similar values for ATP synthase-β on the cell surface of parental and differentiated cells (Fig. 3B).

For OSCP, flow cytometry indicated a significantly more marked ectopic expression in differentiated H9c2 with respect to control cells (Fig. 4A). Confocal microscopy showed a well-defined fluorescent signal symptomatic of plasma membrane localization both in control and in differentiated cells and, when cells were doubly labelled with anti-β and anti-OSCP antibodies, the merged images displayed a yellowish-orange punctuate staining recalling co-localization of the two subunits, that appears to be enhanced in cardiac-like differentiated cells (Fig. 4B). Then we decided to verify the actual assembly of OSCP within the ecto-F_1F_O ATP synthase, and we carried out a protein–protein interaction analysis by *in situ* PLA to get evidence on intact cells. PLA assay is a highly selective and sensitive method for detecting protein–protein interaction and it has been applied to a range of different biological systems [Leuchowius et al., 2010]. Based on the mitochondrial F_1F_O ATP synthase structural data documenting that OSCP interacts at the top of F_1 domain with the subunit α and to a less extent with β [Rees et al., 2009], we probed OSCP interaction with the enzyme using a polyclonal antibody able to recognize α/β subunits. A clear PLA signal visible as distinct florescent green dots was exhibited by only cardiac-like differentiated cells (Fig. 4C), where ecto-OSCP was expressed more than twofold of the parental cells. Thus, taking advantage from the high sensitivity of the method, we can state that such signal is consistent with increased levels

induced by the differentiation of the amount of OSCP really interacting within the enzyme complex. Nevertheless, we cannot rule out improved detection of signal resulting from conformational changes in the enzyme as a possible explanation. Contrary to OSCP, cytofluorimetric analyses for subunits *F6* and *b* showed low immunofluorescence at the surface of H9c2 cells and no increase during differentiation (Fig. 5). The low immunostaining of *F6,* as stated above for ATP synthase-*b*, might be in line with the buried surface area in *b*-*F6* interface, based on the known structure of the peripheral stator stalk of mitochondrial enzyme [Rees et al., 2009; Baker et al., 2012]. Indeed, subunits *F6* and *b* are partially masked by each other, differently from OSCP that sits on top of the F_1 domain.

It is worth mentioning that the F_1F_O ATP synthase mitochondrial biogenesis is reported to involve an assembly from modular sub-assemblies [Fox, 2012], with the two main sub-assemblies expected in membrane being F_1-c ring (containing subunits β) and *a*-*A6L* linked to incomplete stator stalk (containing subunit *b* but not OSCP). On these bases, it may be inferred that the immuno-detection of subunits β and *b*, cannot discriminate between sub-assemblies and assembled enzyme complexes. Conversely, OSCP can be immuno-detected only in the assembled enzyme complex, as the final assembly appears to involve the binding of OSCP, completing the stator stalk, along with the joining of the two sub-assemblies [Fox, 2012]. Based on these considerations, our data might account for the existence of sub-assemblies on the surface of parental H9c2 cells, together with properly assembled F_1Fo complexes, which seem to augment along with the cardiac-like differentiation.

EFFECTS OF THE CARDIAC-LIKE DIFFERENTIATION ON EXATP HYDROLYSIS AND EXATP PRODUCTION BY ECTO-F_1F_O ATP SYNTHASE

As its name implies, OSCP is necessary for F_1F_O ATP synthase to display sensitivity to oligomycin, a well-known inhibitor of the enzyme activity able to prevent the catalytic rotation through its binding to F_O sector, at the interface between the *c*-ring and subunit *a* [Devenish et al., 2000]. The requirement of OSCP probably reflects its important protein–protein interactions made within the assembled complex and transmitted down the peripheral stator stalk, influencing proton channel function and favoring the F_1-F_O coupling. Thus, oligomycin inhibits the ATPase/synthase activity only of the correctly assembled and well coupled F_1F_O complex (holo-F_1F_O ATP synthase). Based on these considerations, we further investigated the possible effect of cardiac-like differentiation of H9c2 on the exATP hydrolysis rate and exATP production by the enzyme at cell surface, focusing in particular on the oligomycin effects.

When we studied the exATP hydrolysis rate, we also used the F_1–targeting inhibitor resveratrol, able to suppress the contribution of uncoupled F_1-F_O complexes and/or sub-assemblies, if there are any, together with that of holo-F_1F_O ATP synthase. Moreover, using resveratrol allowed us to ignore possible intracellular interferences, considering that it was shown to not promptly cross cell membranes [Arakaki et al., 2003]. The results reported in Fig. 6A show that the exATP hydrolysis rate was reduced by more than 75% by 20 μM resveratrol in both parental and cardiac-like differentiated H9c2. Such a marked reduction was elicited also by the antibody for the F_1 catalytic subunit ATP synthase-β, thereby demonstrating low contributions by interferences on cell surface. As the reduction by the antibody resembled the effect of resveratrol, this result validated a good selectivity of resveratrol for the enzyme under our conditions. Thus, the value of exATP hydrolysis rate suppressed by resveratrol was considered as a measure of the enzyme activity at cell surface (ecto-ATPase activity), which resulted to be not significantly different for parental and cardiac-like differentiated cells (13.5 ± 1.5 vs. 12.7 ± 1.4 mU/mg). Conversely, the exATP hydrolysis rate suppressed by oligomycin, estimated as a measure of the ATPase activity of holo-F_1F_O ATP synthase only, was low in parental cells (i.e., 40%) and increased significantly ($P < 0.01$) during the differentiation up to 60% (ecto-ATPase activity taken as 100%) (Fig. 6B). These results indicate that holo-F_1F_O ATP synthase was present at the cell surface of H9c2, it was catalytically competent and augmented in cardiomyocyte-like differentiated cells. Moreover, the finding that a significant portion of the ecto-ATPase activity was insensitive to oligomycin, mainly in the parental cells, suggests that uncoupled complexes and/or sub-assemblies have to be present on the plasma membrane, thus supporting our assumption explaining the immunofluorescence data (see above).

If ecto-F_1F_O ATP synthase is homologous to the mitochondrial enzyme, the holo-enzyme at the cell surface might be able not only to hydrolyse but also to synthesize exATP [Stock et al., 1999], although this aspect is largely debated based on energetic considerations [Mangiullo et al., 2008; Moser et al., 2011; Panfoli et al., 2011; Harris and Attwel, 2012]. Therefore, we thoroughly analyzed exATP production by H9c2 cells, and investigated the effect of the cardiac-likedifferentiating treatment. There are three known enzymes by which exADP may be converted to exATP at the cell surface, specifically adenylate kinase (AK), nucleoside diphosphokinase (NDPK), and F_1F_O ATP synthase; among these AK is recognized to have a prevalent role despite some differences depending on the cell characteristics [Vantourout et al., 2010]. Contrasting with AK and NDPK, F_1F_O ATP synthase requires inorganic phosphate (Pi) to catalyse the ATP synthesis from ADP. Thus, we evaluated the relative contributions of these enzymes based on such substrate specificity, and using a pharmacologic approach with inhibitors. We monitored the exATP production after exposure of intact cells to ADP, or ADP plus Pi, in the absence, or in the presence of oligomycin, or AMP, or UDP, to inhibit the single enzymes selectively (specifically oligomycin to inhibit F_1F_O ATP synthase, AMP to inhibit AK and UDP to inhibit NDPK). For each inhibitor conditions were settled based on inhibitor-titrations experiments (*Supplementary Fig. 4)*, in the range of inhibitory concentrations reported for other cell types [Yegutkin et al., 2001; Fabre et al., 2006; Vantourout et al., 2010]. ATP release from intracellular pool was avoided by accurately monitoring the cell viability for each microplate well (Trypan blue exclusion test, data not shown). In accordance, the level of ATP measured in the absence of exADP was very low (Fig 6C). The exATP generation after adding ADP greatly increased in both parental and differentiated cells (Fig. 6C), indicating that AK represented a major contribution as expected. The addition of ADP+Pi significantly increased (+25%)

the exATP production with respect to ADP alone by cardiac-like differentiated cells only (Fig. 6C, black bars). Based on the Pi substrate specificity, this suggests a role of ectopic holo-F_1F_O ATP synthase in such cells but not in the parental counterpart. In accordance, AMP reduced markedly the exATP production (Fig. 6C inset), confirming a great contribution of AK, which however was not exclusive in cardiac-like differentiated cells, as AMP-inhibition was significantly less (i.e., −65% *vs* −87% in parental cells). Although searching for an explanation for such decrease of AK activity is not the purpose of our work, it may enhance the relative contribution of ectopic holo-F_1F_O ATP synthase in cardiac-like differentiated H9c2 cells. UDP had a less, but still significant effect (Fig. 6C inset), which was not affected by differentiation under our conditions (-22% *vs* −25% in parental cells). Of note, treatment with oligomycin prevented the generation of ADP+Pi-stimulated exATP and reduced (−30%) the conversion of exADP to exATP to the level observed with ADP alone. A similar preventive effect was observed also in the presence of anti-β antibody (−37%), confirming that ADP+Pi-stimulated exATP generation was by ectopic holo-F_1F_O ATP synthase and pointing to a high specificity of oligomycin under our conditions. No effects were elicited on the parental cells either by oligomycin or anti-β antibody. Thus we ascribed to ectopic holo-F_1F_O ATP synthase a different part in the exATP production by the two cell types, that is considerable for cardiac-like differentiated H9c2 cells (black bars), but negligible for parental cells (empty bars). Addition of the protonophore FCCP, known as a mitochondrial uncoupler, suppressed the generation of ADP+Pi-stimulated exATP by differentiated cells and, similarly to oligomycin or anti-β antibody, reduced exATP production (−35%) to a level near to that of ADP alone. In accordance with various reports about different cell types [Arakaki et al., 2003; Mangiullo et al., 2008; Moser et al., 2011; Panfoli et al., 2011; Wang et al., 2012], we consider this clear effect of the protonophore as an evidence for the assumption that the plasma membrane might employ an electrochemical gradient of protons (may be established locally by still unknown pathways) and ectopic holo-F_1F_O ATP synthase to generate exATP. Whether this occurs in heart is unknown, and further investigation is needed to assess the plausibility of this hypothesis.

In summary, the contribution of ectopic holo-F_1F_O ATP synthase to exATP production appears to be significant in cardiac-like differentiated H9c2 only, although to a less extent with respect to AK. Interestingly, although no direct evidence is provided for F_1F_O assembly on the cell surface, the ADP+Pi-stimulated exATP production by ectopic holo-F_1F_O ATP synthase, becomes detectable in concomitance with the increase in OSCP expression and its interaction with α/β subunits. This analysis corroborates in situ PLA results and suggests more well assembled F_1-F_O complexes at the cell surface. Thus, based on the evidence provided by others [Yonally et al., 2006; Wang et al., 2006; Ma et al., 2010; Rai et al., 2013] that makes it unlikely that the enzyme assembles on the plasma membranes, we postulate that sub-assemblies may be transported as holo-F_1F_O ATP synthase from mitochondria to the plasma membranes. Then we may infer that the biogenesis of F_1F_O complexes, that was shown to take place in mitochondria concomitant with the H9c2 cardiac-like differentiation, was able to reduce the presence of sub-assemblies vs. assembled F_1F_O complexes also on plasma membrane, as occurred in mitochondria.

Accordingly, in the parental cells the absence of contribution to exATP production by the holo-enzyme is consistent with the prevalence of sub-assembled/uncoupled complexes; nevertheless, we cannot exclude the involvement of factors reducing exATP generation by the holo-enzyme in such cells.

EFFECTS OF THE CARDIAC-LIKE DIFFERENTIATION ON THE ECTO-F_1F_O ATP SYNTHASE REGULATORY PROTEIN IF_1

Another point that deserves consideration is the possibility that the cardiac-like differentiation may affect the ectopic expression of the regulatory protein ATPase Inhibitory Factor 1 (IF_1), if there is any in embryonic rat heart-derived myoblasts as in endothelial and hepatic cells [Burwick et al., 2005; Cortes-Hernandez et al., 2005; Contessi et al., 2007; Mangiullo et al., 2008]. In order to investigate this aspect, we evaluated by immunofluorescence the ecto-IF_1 expression in parental H9c2 and in differentiated cells. As shown in Fig. 7, IF_1 is actually present on the surface of these cells and differentiation shows a peculiar effect. Cytofluorimetry demonstrated that the IF_1 ectopic expression level was higher in parental than in differentiated cells (Fig. 7A). A greater IF_1/ATP synthase-β ratio was inferred for parental cells with respect to cardiac-like differentiated cells, due to the significant difference of IF_1 expression compared to the equal levels of its natural target ATP synthase-β at the cell surface. Confocal microscopy showed a good co-localization of IF_1 with ATP synthase-β (merged images), which appeared to be more intense in parental cells (Fig. 7B). The analysis by in situ PLA documented that a signal, visible as distinct florescent green dots, was exhibited only by parental cells (Fig. 7C), suggesting that in this case IF_1 really interacts with ATP synthase-β at the cell surface.

These data are consistent with a higher binding of the regulatory protein IF_1 to its target subunit β within the enzyme complexes on the surface of parental proliferating H9c2, thereby evoking a more strictly regulatory role in these cells with respect to cardiac-like differentiated cells. Based on the known properties of IF_1 binding to mitochondrial F_1F_O ATP synthase [Green and Grover, 2000; Bason et al., 2011] and considering our data about the enzyme activity on the surface of the parental cells (i.e., low sensitivity to oligomycin and undetectable generation of ex-ATP), we postulate that more regulation by IF_1 might be required by the presence on the surface of the parental cells of smaller quantity of holo-F_1F_O ATP synthase and greater quantity of sub-assemblies. Of note, in agreement with our hypothesis are the previous reports revealing in different models of genetic disorders a great IF_1 quantity associated to F_1F_O ATP synthase sub-assemblies in mitochondrial membrane [Carrozzo et al., 2006; Mourier et al., 2014]. To reinforce our evidence we exposed the parental myoblasts to lower pH, considering that decrease of pH favors IF_1 binding to ATP synthase. Under conditions mimicking acidosis without affecting cell viability (i.e., pH 7.0), the ATPase activity of the enzyme at the cell surface was 20% lower than at pH 7.4 (results not show), supporting our hypothesis that endogenous IF_1 is able to regulate the enzyme at the cell surface of myoblasts.

The relevance of our study is in the fact that few reports provided evidence for an inhibitory effect elicited by endogenous IF_1 on the enzyme on the cell surface [Cortes-Hernandez et al., 2005; Contessi et al., 2007; Mangiullo et al., 2008; Giorgio et al., 2010; Ravera et al., 2011; Martinez et al., 2015], and none was in the context of cardiac-like differentiation.

CONCLUDING REMARKS

The present study is the first to demonstrate that holo-F_1F_O ATP synthase was expressed on the plasma membranes of embryonic rat heart-derived myoblasts, also showing that it increased along with cardiac-like differentiation, as occurs in mitochondria. As a matter of fact, the results of the functional measurements together with the *in situ* PLA data for OSCP corroborate the hypothesis of a higher expression of ecto-F_1F_O complexes that were properly assembled/coupled on the surface of cardiac-like differentiated cells. Of note, a contribution of F_1F_O ATP synthase to the exATP production (specifically ADP+Pi-stimulated exATP generation) was observed in differentiated cells. Conversely, in the parental counterpart the finding that exATP hydrolysis ascribed to the enzyme was largely oligomycin-insensitive is in line with the deficit of OSCP and suggests the occurrence of sub-assemblies. Overall, our results are consistent with the hypothesis that plasma membrane can reflect the forms resident inside mitochondrial membrane and the modifications occurring during cardiac-like differentiation and enzyme complex biogenesis. It is difficult to exclude based on our data that the plasma membrane localization of the enzyme complex is just an aberration of cell trafficking in a cultured cell line. Nevertheless, one may infer that it is not the case based on evidence from different laboratories on i) rat liver plasma membranes [Giorgio et al., 2010; Raj et al., 2013], ii) rat liver *ex vivo* [Martinez et al., 2003], iii) mice liver in vivo [Song et al., 2014]. Further investigations on heart are needed. Notably, the expression of ecto-IF_1 was reduced by differentiation opposed to OSCP, and the interaction of IF_1 with ATP synthase-β observed at the cell surface suggests that it might regulate the prevailing exATP hydrolysis by the enzyme in parental cells (at least partially due to sub-assemblies).

Defining the role of the enzyme on the plasma membrane of H9c2 cells is out of the purpose of our work. Several laboratories largely investigated the role of the enzyme on endothelial and tumoral cells, hepatocytes, adipocytes, myotubes [Vantourout et al., 2010 and references therein], as well as in developing muscle cells [Garcia al., 2011] and neural cells [Xing et al., 2012]. Hence, it is now accepted that cell surface ATP synthase likely functions as a cell surface receptor for a number of ligands triggering hydrolysis or synthesis of ATP in the extracellular milieu. In that way, it regulates H^+ concentration across the membrane and affects purinergic signaling [Chi et al., 2006; Vantourout et al., 2010]. The more studied ligands are: angiostatin [Moser et al., 2011], coupling factor 6 [Osanai et al., 2012], apoliporotein A–I (ApoA–I) [Martinez et al., 2015], oligomeric amyloid-β peptide (Aβ) and the amyloid precursor protein [Xing et al., 2012], α2/δ1 subunit of calcium channels [Garcia al., 2011]. Consequently, cell surface ATP synthase seems to be involved in processes as angiogenesis, vascular tone, cholesterol, and lipoprotein metabolism [Chi et al., 2006; Kim et al., 2010], calcium release regulation especially during early development of myotubes [Garcia al., 2011], oligomeric Aβ neurotoxic effects and neurodegeneration [Xing et al., 2013]. Thus, the emerging idea is that cell surface ATP synthase may be an intervening target of pathogenesis of several diseases (e.g., cancer, atherosclerosis, hypertension, and lipid disorders, Alzheimer disease). In this scenario, it is tempting to postulate two of the roles mentioned above as more likely to be played by the enzyme in H9c2 cells, considering that i) the regulation of Ca^{2+} homeostasis in cardiomyocytes is crucial as in myotubes, α2/δ1 subunits are the same in both cardiac and muscle calcium channels [Kamp and Hell, 2000] and the expression of L-type Ca^{2+} channel was shown to be promoted in H9c2 by the cardiomyocyte-like differentiation [Menard et al., 1999], ii) cardiac amyloidosis is a rare but known cause of cardiomyopathies, and mainly disorders of the conduction system and valves [Falk andDubrney, 2010].

ACKNOWLEDGMENT

We are thankful to Dr. Guy Waley for proofreading the English language of the manuscript. This work was supported by University of Udine.

REFERENCES

Arakaki N, Nagao T, Niki R, Toyofuku A, Tanaka H, Kuramoto Y, Emoto Y, Shibata H, Magota K, Higuti T. 2003. Possible role of cell surface H^+-ATP synthase in the extracellular ATP synthesis and proliferation of human umbilical vein endothelial cells. Mol Cancer Res 1:931–993.

Bae TJ, Kim MS, Kim JW, Kim BW, Choo HJ, Lee JW, Kim KB, Lee CS, Kim JH, Chang SY, Kang CY, Lee SW, Ko YG. 2004. Lipid rafts proteome reveals ATP synthase complex in the cell surface. Proteomics 4:3536–3548.

Baker LA, Watt IN, Runswick MJ, Walker JE, Rubinstein JL. 2012. Arrangement of subunits in intact mammalian mitochondrial ATP synthase determined by cryo-EM. PNAS 10:11675–11680.

Bason JV, Runswick MJ, Fearnley IM, Walker JE. 2011. Binding of the Inhibitor Protein IF_1 to Bovine F_1-ATPase. J Mol Biol 406:443–453.

Bisetto E, Comelli M, Salzano AM, Picotti P, Scaloni A, Lippe G, Mavelli I. 2013. Proteomic analysis of F_1F_O-ATP synthase super-assembly in mitochondria of cardiomyoblasts undergoing differentiation to the cardiac lineage. Biochim Biophys Acta 1827:807–816.

Carrozzo R, Wittig I, Santorelli FM, Bertini E, Hofmann S, Brandt U, Schagger H. 2006. Subcomplexes of human ATP synthase mark mitochondrial biosinthesis disorders. Ann Neurol 59:265–275.

Chi SL, Pizzo SV. 2006. Cell surface F_1F_O ATP synthase: A new paradigm?. Ann Med 38:429–438.

Comelli M, Domenis R, Bisetto E, Contin M, Marchini M, Ortolani F, Tomasetig L, Mavelli I. 2011. Cardiac differentiation promotes mitochondria development and ameliorates oxidative capacity in H9c2 cardiomyoblasts. Mitochondrion 11:315–326.

Comelli M, Metelli G, Mavelli I. 2007. Downmodulation of mitochondrial F0F1 ATP synthase by diazoxide in cardiac myoblasts: A dual effect of the drug. Am J Physiol Heart Circ Physiol 292:H820–H829.

Contessi S, Comelli M, Cmet S, Lippe G, Mavelli I. 2007. IF(1) distribution in HepG2 cells in relation to ecto-F(0)F(1)ATPsynthase and calmodulin. J Bioenerg Biomembr 39:291–300.

Cortes-Hernandez P, Dominiguez-Ramirez L, Estrada-Berna A, Montez-Sanchez DG, Zentella-Dehesa A, deGomez-Puyou MT, Gomez-Puyou A, Garcia JH. 2005. The inhibitor protein of the F_1F_O-ATP synthase is associated to the external surface of endothelial cells. Biochim Biophys Res Commun 330:844–849.

Daubney J, Bonner PL, Hatgreaves AJ, Dickenson JM. 2015. Cardioprotective and cardiotoxic effects of quercetin and two of its in vivo metabolites on differentiated H9c2 cardiomyocytes. Bas Clin Pharmacol Toxicol 116:96–109.

Devenish RJ, Prescott M, Boyle GM, Nagley GM. 2000. The oligomycin axis of mitochondrial ATP synthase: OSCP and the proton channel. J Bioenerg Biomembr 32:507–515.

Fabre ACS, Vantourout P, Champagne E, Tercè F, Rolland C, Perret B, Collet X, Barbaras R, Martinez LO. 2006. Cell surface adenylate kinase activity regulates the F1-ATPase/P2Y/13)-mediated HDL endocytosis pathway on human hepatocytes. Cell Mol Life Sci 63:2829–2283.

Falk RH, Dubrey SW. 2010. Amyloid heart disease. Prog Cardiovasc Dis 52:347–361.

Fox TD. 2012. Mitochondrial protein synthesis, import, and assembly. Genetics 192 1203–1234.

Garcia J. 2011. The calcium channel a2/≐1 subunit interacts with ATP5b in the plasma membrane of developing muscle cells. Am J Physiol Cell Physiol 301:C44–C52.

Giorgio V, Bisetto E, Franca R, Harris DA, Passamonti S, Lippe G. 2010. The ectopic F(0)F(1) ATP synthase of rat liver is modulated in acute cholestasis by the inhibitor protein IF1. J Bioenerg Biomembr 42:117–123.

Green DW, Grover GJ. 2000. The IF(1) inhibitor protein of the mitochondrial F (1)F(0)-ATPase. Biochim Biophys Acta 1458:343–355.

Harris JJ, Attwel D. 2012. Is myelin a mitochondrion?. J Cerebral Blood Flow Metab 1–4.

Hescheler J, Meyer R, Plant S. 1991. Morphological, biochemical, and electrophysiological characterization of a clonal cell (H9c2) line from rat heart. Circulation Res 69:1476–1486.

Jurisic V. 2003. Estimation of cell membrane alteration after drug treatment by LDH release. Blood 101:2894.

Jurisic V, Bumbasirevic V, Konjevic G, Djuricic B, Spuzic I. 2004. TNF-alpha induces changes in LDH isotype profile following triggering of apoptosis in PBL of non-Hodgkin′s lymphomas. Ann Hematol 83:84–91.

Kamp TJ, Hell JW. 2000. Regulation of cardiac L-type calcium channels by protein kinase A and protein kinase C. Circ Res 87:1095–1102.

Kim BW, Lee CS, Yi JS, Lee JH, Lee JW, Choo HJ, Yung SY, Kim MS, Lee SW, Lee MS, Yoon G, Ko Y. 2010. Lipid raft proteome reveals that oxidative phosphorylation system is associated with the plasma membrane. Expert Rev Proteomics 7:849–866.

Kuznetsov AV, Javadovb S, Sickinger S, Frotschnig s, Grimm M. 2015. H9c2 and HL-1 cells demonstrate distinct features of energy metabolism, mitochondrial function and sensitivity to hypoxiareoxygenation. Biochim Biophys Acta 1853:276–284.

Leuchowius KJ, Jarvius M, Wickstrom M, Rickardson L, Landegren U, Larsson R, Soderberg O, Fryknas M, Jarvius J. 2010. High content screening for inhibitors of protein interaction and post-translational modifications in primary cells by proximity ligation. Mol Cell Proteomics 9:78–183.

Ma Z, Cao M, Liu Y, He Y, Wang Y, Yang C, Wang W, Zhou YDM, Gao F. 2010. Mitochondrial F_1F_O-ATP synthase translocates to cell surface in hepatocytes and has high activity in tumor-like acidic and hypoxic environment. Acta Bioch Biophys Sin 242:530–537.

Mangiullo R, Gnoni A, Leone A, Gnoni GV, Papa S, Zanotti F. 2008. Structural and functional characterization of F_0F_1-ATP synthase on the extracellular surface of rat hepatocytes. Biochim Biophys Acta 1777:1326–1335.

Martinez LO, Jacquet S, Esteve JP, Rolland C, Cabezón E, Champagne E, Pineau T, Georgeaud V, Walker JE, Tercé F, Collet X, Bertrand Perret B, Barbara R. 2003. Ectopic β-chain of ATP synthase is an apolipoprotein A-I receptor in hepatic HDL endocytosis. Nature 421:75–79.

Martinez LO, Najib S, Perret B, Cabou C, Lichtenstein L. 2015. Ecto-F1-ATPase/P2Y pathways in metabolic and vascular functions of high density lipoproteins. Atherosclerosis 238:89–100.

Menard C, Pupier S, Mornet D, Kitzmann M, Nargeot J, Lory P. 1999. Modulation of L-type calcium channel expression during Retinoic acid-induced differentiation of H9C2 cardiac cells. J Biol Chem 274:29063–29070.

Moser TL, Kenan DJ, Ashley TA, Roy JA, Goodman MD, Misra UK, Cheek DJ, Pizzo SV. 2011. Endothelial cell surface F_1-F_O ATP synthase is active in ATP synthesis and is inhibited by angiostatin. Proc Natl Acad Sci USA 98:6656–6661.

Mourier A, Ruzzenente B, Brandt T, Kühlbrandt W, Larsson N. 2014. Loss of LRPPRC causes ATP synthase deficiency. Hum Mol Genet 23:2580–2592.

Osanai T, Tanaka M, Magota K, Tomita H, Okumura K. 2012. Coupling factor 6-induced activation of ecto-F1F(o) complex induces insulin resistance, mild glucose intolerance and elevated blood pressure in mice. Diabetologia 55:520–529.

Panfoli I, Ravera S, Bruschi M, Candiano G, Morelli A. 2011. Proteomics unravels the exportability of mitochondrial respiratory chain. Exp Rev Proteomics 8:231–239.

Pereira SL, Ramalho-Santos J, Branco AF, Sardao VA, Oliveira PJ, Rui AC. 2011. Metabolic remodeling during H9c2 myoblast differentiation: Relevance for in vitro toxicity studies. Cardiovasc Toxicol 11:180–190.

Rai AK, Spolaore B, Harris DA, Dabbeni-Sala F, Lippe G. 2013. Ectopic F_0F_1 ATP synthase contains both nuclear and mitochondrially-encoded subunits. J Bioenerg Biomembr 45::569–579.

Ravera S, Panfoli I, Aluigi MG, Calzia D, Morelli A. 2010. Characterization of myelin sheath F(o)F(1)-ATP synthase and its regulation by IF (1). Cell Biochem Biophys 59:63–70.

Rees DM, Leslie AG. 2009. The structure of the membrane extrinsic region of bovine ATP synthase. Proc Natl Acad Sci USA 106:21597–21601.

Song K, Han Y, Zhang L, Liu G, Yang P, Cheng Y, Bu L, Sheng H, Qu S. 2014. ATP synthase β-Chain overexpression in SR-BI knockout mice increases HDL uptake and reduces plasma HDL level. Int J Endocrinol 356432:1–12.

Stock D, Leslie AG, Walker JE. 1999. Molecular architecture of the rotary motor in ATP synthase. Science 286:1700–1705.

Vantourout P, Radojkovic C, Lichtenstein L, Pons V, Champagne E, Martinez LO. 2010. Ecto-F_1-ATPase: A moonlighting protein complex and an unexpected apoA-I receptor. World J Gastroenterol 16:5925–5935.

Wang T, Chen Z, Wang X, Shyy JY, Zhu Y. 2006. Colesterol loading increases the translocation of ATP synthase b chain into membrane caveole in vascular endothelial cells. Biochim Biophys Acta 1761:1182–1190.

Wang WJ, Ma Z, Liu YW, He YQ, Wang YZ, Yang CX, Du Y, Zhou MQ, Gao F. 2012. A monoclonal antibody (Mc178-Ab) targeted to the ecto-ATP synthase β-subunit-induced cell apoptosis via a mechanism involving the MAPKase and Akt pathways. Clin Exp Med 12:3–12.

Wang WJ, Shi XX, Liu YW, He YQ, Wang YZ, Yang CX, Gao F. 2013. The mechanism underlying the effects of the cell surface ATP synthase on the regulation of intracellular acidification during acidosis. J Cell Biochem 114:1695–1703.

Xing SL, Chen B, Shen DZ, Zhu CQ. 2012. β-amyloid peptide binds and regulates ectopic ATP synthase α-chain on neural surface. Int J Neurosci 122:290–297.

Xing S, Shen D, Chen C, Wang J, Liu T, Yu Z. 2013. Regulation of neuronal toxicity of β-amyloid oligomers by surface ATP synthase. Mol Med Rep 8:1689–1694.

Yegutkin G, Henttinen T, Jalkanen S. 2001. Extracellular ATP formation on vascular endothelial cells is mediated by ecto-nucleotide kinase activities via phosphotransfer reactions. FASEB J 15:251–260.

Yonally SK, Capaldi RA. 2006. The F_1F_O ATP synthase and mitochondrial respiratory chain complexes are present on the plasma membrane of an osteosarcoma cell line: An immnocytochemical study. Mitochondrion 6:305–314.

SUPPORTING INFORMATION

Additional supporting information may be found in the online version of this article at the publisher′s web-site.